Preparation of TiO_2 Coatings on PET Monoliths for the Photocatalytic Elimination of Trichloroethylene in the Gas Phase

Benigno Sánchez[a*], *Juan M. Coronado*[a], *Roberto Candal*[b], *Raquel Portela*[a], *Isabel Tejedor*[c], *Marc A. Anderson*[c], *Dean Tompkins*[c] *and Timothy Lee*[c]

a) Aplicaciones Ambientales de la Radiación Solar. CIEMAT. Av Complutense, 22, Building 42. Madrid. Spain.

b) INQUIMAE Ciudad Universitaria Pab. 2, 1428 Buenos Aires. Argentina.

c) Environmental Chemistry & Technology Program. University of Wisconsin at Madison. 660 North Park Street. Madison. WI 53706. USA.

Keywords: Photocatalysis, TiO_2, coating, polymers, PET, monoliths, TCE, SEM

[*] Corresponding author. Email: benigno.sanchez@ciemat.es. Phone: +34913466417 Fax :+34913466037

Abstract

This paper presents the first data on the performance of polyethylene terephthalate (PET) monoliths as photocatalytic support. For this purpose, first a protective layer of SiO_2 was applied to the polymer to prevent oxidation of the substrate, and subsequently the photoactive layer of TiO_2 was deposited on PET monoliths using the dip-coating technique. In order to increase adherence of the inorganic coatings, two different synthesis procedures were evaluated. One approach was based on reducing the surface tension of the SiO_2 sol using a fluorinated surfactant to increment the PET wettability. The second approach consisted in modifying the PET surface with a layer of the polymer poly(diallyldimethylammonium) chloride (PDDA), which provides a positively charged surface for the fixation of the alkaline SiO_2 sol. Both TiO_2/SiO_2 coated PET monoliths were assayed in a single-pass annular reactor for the destruction of trichloroethylene (TCE). The two coating procedures were compared in terms of homogeneity, durability and photocatalytic activity.

Keywords: photocatalysis, TiO_2, coating, polymers, PET, monoliths, TCE, SEM

1. Introduction

Optimization of light harvesting is among the main concerns in photocatalysis, and consequently a considerable effort has been devoted to designing photoreactors that provide efficient illumination of the photocatalyst [1-3]. Similarly, the development of materials, which can provide a strong absorption of the available photons, has attracted a great deal of interest [3, 4]. In this context, the use of TiO_2 thin films deposited on transparent supports reduce shading and allow photoactivation of the whole coating. This fact result in a superior performance of TiO_2 thin films for the removal of organic vapors when compared with the same material in the form of pellets or powders [4]. On the other hand, supported photocatalysts can be employed for continuous processes, such as those required for the treatment of gas effluents [2].

In most studies, borosilicate glass has been utilised as photocatalytic support, because it provides good adherence and an appropiate transparency window (ca. 400-330 nm) for TiO_2 activation [3, 5]. The use of organic polymers with high transmittance in the UVA region as substrates could be advantageous for certain applications, because plastics are lightweight materials and can easily be shaped in a variety of geometries. Consequently, the preparation of inorganic thin films on organic supports is currently attracting a significant attention [6-9]. Monoliths are the most suitable configuration for treating large volumes of gaseous effluents, because they cause a small pressure drop. Until now, only ceramic monoliths have been used in gas photocatalysis, with the drawback of the channel walls opacity [10]. In contrast, transparent polymer monoliths could enable efficient irradiation, in a perpendicular direction to the gas flow.

The deposition of TiO_2 coatings on plastic substrates presents several difficulties that should be adequately addressed before it can be used as photocatalyst. First, TiO_2 film adhesion to the polymer is usually poor, and therefore modification of the organic surface may be necessary [7]. Second, well crystallized TiO_2 particles are required in order to achieve optimal photocatalytic performance, but ordered domains are usually obtained at high treatment temperatures, which are not compatible with thermally sensitive substrates [6, 8]. Finally, photo-oxidation of the polymeric support must be avoided because it could reduce the transparency and the mechanical resistance of these materials [11].

In this work, we have prepared TiO_2 thin-film coatings on transparent polyethylene terephthalate (PET) monoliths by a sol-gel procedure, and evaluated their performance in the photocatalytic removal of trichloroethylene (TCE). A layer of SiO_2 was placed sandwich-like between the organic surface and the photocatalytic film in order to prevent photooxidation of the polymeric support. Adherence of the inorganic oxides to the polymer surface was promoted in two different ways: i) a fluorinated surfactant was added to the SiO_2 sol to increase wettability, or ii) the monoliths were first immersed in a poly(diallyl-dimethyl-ammonium chloride) (PDDA) aqueous solution to form a polar film to increase interaction with colloids. In all cases, the inorganic coating was fixed by drying at 60ºC to prevent deterioration of the PET monolith.

2. Experimental

2.1. Preparation of the coatings

TiO_2 and SiO_2 were synthesized by sol-gel processing (for a detailed description see ref [11]). An acidic TiO_2 sol was prepared by adding $Ti(OPr^i)_4$ (97 %, Aldrich) to an aqueous

solution of nitric acid, which was subsequently stirred at room temperature until total peptization. Basic SiO_2 sol was prepared by adding $Si(OEt)_4$ (98 %, Aldrich) to an aqueous solution of ammonium hydroxide and stirred until total peptization. The acid and basic sols were dialyzed to a final pH of 3.4 or 8.0 respectively, using deionized cellulose membranes.

Polyethylene terephthalate (PET) monoliths, primarily used as thermal insulators in passive solar systems, were provided by Wacotech GmbH & Co. KG (Bielefeld, Germany). The polymeric monoliths, which have a geometric surface area of 2.23 m^2/m^3, pitch cross-section of 10 mm x 10 mm, wall thickness of 0.1 mm and density of 45 Kg/m^3 were thoroughly washed with deionized water and dried before TiO_2 was deposited by dip-coating with a withdrawal rate of 4 $mm.s^{-1}$.

A first series of SiO_2 coated monoliths (*Procedure A*) was prepared using the SiO_2 sol modified with a surfactant based on perfluorobutane sulfonate (FC-4430 provided by 3M Corporation) dissolved in 2-propanol and added in the amount required to obtain a concentration of 25 mg/L. After coating, the monoliths were dried first at room temperature (c.a. 22 ºC, 30% RH) and then at 60 ºC for 60 minutes. A second layer of SiO_2 was deposited following the same procedure.

Another set of clean monoliths (*Procedure B*), were submerged in a 1 % v/v aqueous solution of poly(diallyl-dimethyl-ammonium chloride) (PDDA, low molecular weight (100000-200000 Da) 20% solution in water supplied by Aldrich) for two minutes, then rinsed with deionized water and, once dried at room temperature (c.a. 22 ºC, 30% RH), coated with the unmodified SiO_2 sol. After this process, the PET surface is expected to acquire a positive charge due to the $CH_3\text{-}N^+(R)_4$ groups of adsorbed PDDA. Later, the monoliths were coated with two layers of SiO_2 in the same conditions as in the previous case, but the sol used did not contain any surfactant. Finally, four layers of photoactive TiO_2 were deposited on the

SiO_2/PET monoliths prepared according to each procedure, following the same dip-coating and drying protocol.

2.2. Materials Characterization

Powder XRD patterns of ground xerogels were recorded on a Seifert XRD 3000P diffractometer using nickel-filtered Cu k_α radiation. The UV-Visible absorption spectra of sols were recorded on a HP8452A diode array spectrophotometer, using air as reference. The morphology of the coating was studied with a Zeiss DSM 960 Digital Scanning Microscope coupled with an analyzer of dispersive energies EDX Link eXL. Samples were initially coated with a conductive layer of graphite for the analysis.

Monoliths samples were artificially weathered in an accelerated weathering chamber QUV (The Q panel Company) following the ASTM G53-88 norm. This instrument is provided with 8 UVB fluorescent lamps of 40 W with maximum emission at 313 nm, and submits the samples to continuous cycles of irradiation (4 hours at 60ºC) and water condensation (4 hours at 50ºC).

2.3 Photocatalytic Activity Measurements

The photocatalytic oxidation of trichloroethylene (TCE) was studied in a continuous plug flow gas-phase photoreactor consisting of a Pyrex glass cylinder in which four coated PET monoliths were fitted. A scheme of the experimental set-up along with a picture of the photocatalytic reactor is displayed in Figure 1. Illumination was provided by a UVA 8W Sylvania fluorescent lamp, which presents a maximum emission at 365 nm; it was placed in

axial position along the reactor. A stream from a calibrated cylinder containing 252 ppmv of TCE in N_2 was mixed with the adequate flow of dry air to obtain a final mixture with a concentration of 30, 81 or 142 ppmv of the pollutant. The flow rate was established using electronic mass flow controllers and the oxygen content of the mixture fed to the photoreactor varied from 15 to 20%.

Reaction products were analyzed in a Varian CP-4900 Micro-GC equipped with a Thermal micro-conductivity detector (μ-TCD) and column 10 m x 0.15 mm CP-PoraPlot Q. In addition, in order to identify the intermediate reaction products, selected experiments were monitored using a multiple reflection gas cell (2 m path length, provided by Thermo) and a FTIR Thermo-Nicolet 5700 spectrometer. A detailed description of the set-up used for photocatalytic measurements can be found elsewhere [10].

3. Results and Discussion

3.1. Characterization of the TiO_2 coated PET monoliths

TiO_2 xerogels, obtained from the same sol used to coat the PET monoliths dried at 60ºC, consist of anatase crystallites with a minor brookite contribution, according to XRD data shown in Figure 2. The weight ratio between anatase and brookite is 90:10, as it can be calculated using the equation proposed by H. Zhang and J. F. Bandfield [12] from the area of the most intense peaks of anatase ((101) reflection; 2θ=25.35º) and brookite ((121) reflection; 2θ=30.81º). The mean crystalline size was estimated to be 4 nm by the Scherrer equation. Therefore, as previous studies have shown [13, 14], acidic peptization and aging of the TiO_2 sol allows to obtain nanocrystalline anatase at low temperatures.

Procedure A yields a very uneven coating of PET, which is formed by oxides particles dispersed on the polymer surface, as shown in Figure 3A. The particle size distribution is rather wide as agglomerates with diameter ranging from 1 to 200 μm can be detected. Nevertheless, most of the particles are smaller than 10 μm. XEDS analysis of these deposits confirms that most of the TiO_2 is concentrated there. The average atomic ratio of Ti (referred to the total amount of metals detected) is 0.08 but it ranges from area to area between 0.26 and 0.02 (see Figure 4). In contrast, the distribution of SiO_2 is more difficult to determine because the PET substrate also contains a silicate of aluminum and magnesium and, consequently, a silicon signal can be obtained all along the polymer surface. Yet, the noticeable increment in the Si/Mg ratio from 1.6 in untreated PET to 8.6 in the sample coated by Procedure B, reveals that SiO_2 is also deposited in these samples. In addition, Si seems to be more uniformly distributed than Ti, as its atomic ratio is rather constant in all analyzed areas. These results can be interpreted considering that, although the SiO_2 sol containing the surfactant wets well the PET surface yielding a relatively uniform layer, the subsequent interaction of this coating with the TiO_2 sol is not as favorable, and consequently particles rather than a film are formed.

Monoliths prepared according to Procedure B have a remarkably different morphology, as it is shown in Figure 3C. PDDA deposition results in a cracked film, which covers almost the entire PET surface (see Figure 3B). The addition of SiO_2 and TiO_2 does not modify significantly this morphology. The presence of oxide particles is not obvious in the SEM micrographs, although the border of cracks is a more jagged in presence of the metal oxides (see Figure 3B and C), and this could indicate certain accumulation of SiO_2 and TiO_2 on these areas. In any case, these results indicate oxides particles are basically below the resolution limit of the SEM. Yet, XEDS analysis (see Figure 4B) reveal that both Ti and Si are well distributed on the PET surface, because these element are detected in similar

proportion in all analyzed areas. Comparison with the results obtained with A monoliths, shows that on average the Si concentration is slightly lower (Si/Mg =3.9) for the coatings prepared by procedure B, although it is still notably higher than the uncovered PET. In contrast the average Ti atomic ratio is 0.27, which is about 3.5 times larger than the concentration found in A monoliths. This rather high homogeneous distribution of TiO_2 in B type monoliths is very likely related to the presence of CH_3-$N^+(R)_4$ groups in the PDDA film, which first favor the anchoring of negatively charged SiO_2 particles (basic sol), and subsequently allow the attachment of TiO_2 crystallites. Nevertheless, preparation of crack free TiO_2 thin-films on polymer substrates still remains as a challenge, because it requires a very precise control of all the synthesis parameters [15].

On the other hand, after reaction with TCE a certain amount of chlorine associated with TiO_2 is detected on the monoliths prepared by both methods. An example of these analysis is displayed in of Figure 4B, which shows the spectrum of B monoliths used in reaction. The presence of chlorine can be ascribed to either adsorbed TCE or chlorinated intermediate species produced during the photodegradation, which have been also detected by FTIR on the surface of nanostructured TiO_2 [16].

Figure 5 shows the UV-vis transmittance spectra of the PET monoliths, both uncoated and after formation of the photocatalytic layer. The PDDA layer slightly reduces the transmittance of the PET support, but does not generate any additional feature in the spectrum. In contrast, TiO_2 coatings cause a small but significant decrease in transmittance in the 320-350 nm range, which can be associated with the band-gap absorption of this semiconductor [17, 18]. It is interesting to note that the transmittance in this range is lower for the monoliths prepared by Procedure B. These results are qualitatively in accordance with the XEDS results, which indicate that B monoliths have a higher TiO_2 content. On the other hand, an absorption coefficient of 4.6 10^6 m^{-1} was determined for TiO_2 using thin films of

known thickness prepared by a similar sol-gel procedure on borosilicate glass. This value is consistent with literature values [18], and it allows to give a rough estimation of the coating thickness. Thus, assuming that the TiO_2 layers deposited on PET monoliths are uniform, coatings prepared by procedure A are 40 nm thick, while coatings prepared by procedure B present a thickness of 95 nm. Nevertheless, considering the roughness and heterogeneity of the layers, these figures can be only taken as a crude approximation of the width of TiO_2 coating deposited on the PET substrate.

PET, as many other polymers, can be damaged by UV radiation due to photochemical oxidation, which induces the breakage of the ester bonds and leads to the formation of a number of degradation products (hydroperoxides, carboxylic acids…) [19]. Therefore, it is important to determine the influence of the TiO_2/SiO_2 coating in the long term stability of the PET monoliths. For this purpose, unmodified and coated PET monoliths were treated in a weathering chamber for accelerated aging. Photo-oxidation process can be monitored spectroscopically, since degradation of the polymer changes the transmittance in the UV-vis, In particular, the spectrum of weathered PET is characterized by the formation of new band centered about 330 nm [19], and this feature has been selected in the present study to evaluate the degree of aging. Figure 6 displays the lost of transmittance at 330 nm for the three analyzed samples with the time of treatment. These results show that coated and uncoated monoliths present a very similar behavior, with an almost exponential drop in transmission. The stability of A type and uncoated PET monoliths is very similar, while the degradation rate of B monoliths is slightly faster. In any case, the presence of TiO_2 seems to exert a minor influence in the durability of these materials, very likely due to the barrier effect of the SiO_2 layer. In any case, as these photoactive materials are expected to operate at less stringent conditions than those using in accelerated aging (e.g. using UVA instead of UVB light for excitation), photo-oxidation of PET in practical applications could be limited.

3.2 Photocatalytic Activity of TiO_2 coated PET Monoliths for TCE elimination

Figure 7 shows the variation in TCE conversion as a function of the residence time for different initial concentrations of pollutant using monoliths prepared by Procedures A and B. The high TiO_2 coated PET monolith performance for TCE degradation suggests that firing of the TiO_2 layer is not necessary to obtain active photocatalysts, as long as anatase crystallites are already formed in the sol.

As expected, efficiency in TCE destruction increases with increasing residence time and decreasing TCE concentration in the inlet flow. These results can be rationalized considering the design equation for a fixed bed plug flow reactor

$$\frac{W}{F} = \int \frac{dX}{r}$$

where W is the catalyst weight, F is the flow rate, X the fraction of TCE degraded, and r the reaction rate. Using this expression, and assuming that the TCE degradation rate follows a first order kinetic, as found in other studies [20], the following expression can be obtained:

$$- (k\, C_0\, W\, \tau)/ V = \ln(1-X)$$

where C_0 is the TCE concentration in the inlet stream, k is the kinetic constant, V the volume of the monolith and τ the residence time. The least square fitting of the experimental data to this equation are plotted in Figure 7 as solid lines, and it shows a satisfactory correlation (r=0.99-0.94). These results indicate that TCE photocatalytic degradation on these monoliths can be adequately modelled assuming a first order kinetic. These results can be rationalized based on the Langmuir-Hinshelwood model. Under our experimental conditions (low partial pressures of TCE) the amount of TCE adsorbed on the TiO_2 coating is rather low, leading to

lower coverages (θ_{TCE} <<1). In these cases, the L-H model can be approximated by a first order kinetic [20]. In any case, results of Figure 7 indicate that monoliths prepared by Procedure B are slightly more photoactive than those prepared using Procedure A. Consequently, the kinetic constant, k, obtained from the fitting of the data to the model is about 1.2 times larger for the TiO_2/PDDA/PET monoliths. These differences can be related to the larger amount of TiO_2 deposited over the PDDA layer, although according to the XEDS data a larger increment should be expected. This fact suggests that part of the TiO_2 may not be accessible to reactants and/or photons.

Progress of CO_2 production and TCE removal under UVA illumination using monoliths prepared with Procedure B are shown in Figure 8. These results confirm that at high residence time (τ = 21 s) the TCE can be totally removed from the gas stream. FTIR analysis of the effluent gases also shows the formation of small amount of dichloroacetyl choride (DCAC), CO, $COCl_2$ and HCl. Nevertheless, CO_2 accounts for more than 95 % of the carbon balance, and may therefore be concluded that, as previously found [21], for long residence times, CO and $COCl_2$ are only present as traces. In addition, the inclusion of steam in the feed flow leads to an additional decrease in phosgene production, in agreement with previous studies [22]. Finally, it is worth noting that, although further studies are required to establish the long-term stability of the photoactivity of these materials, monoliths have been assayed in different conditions for more than for 12 hours without suffering deactivation.

Conclusions

This study has shown that UV-transparent PET monoliths can be effectively employed as photocatalytic supports. These materials present a high photocatalytic activity for the degradation of TCE and provide an opportunity for developing very light-weight, low-cost photocatalytic reactors with a small pressure drop. Photodegradation of these materials occurs

under UVB irradiation, but the rate is expected to be relative low at normal operation conditions. Nevertheless, additional work is required to explore new methods of synthesis, which allow to improve coating homogeneity and cristallinity of the deposited TiO_2.

Acknowledgments

This work has been partially founded by MEC (Spain); project number CTQ2004-08232-CO2-01/PPQ. CONICEP (PIP 5215) and ANPCyT (PICT 10621). Argentina. RJC is member of CONICET

References

~~1.~~[1] C. Guillard, J. Disdier, C. Monnet, J. Dussaud, S. Malato, J. Blanco, M. I. Maldonado, J.M. Herrmann, Appl. Catal. B, 46, (2003), 319

~~2.~~[2] M. Romero, J. Blanco, B. Sánchez, A. Vidal, S. Malato, A. I. Cardona, E. García, Solar Energy, 66 (1999) 169

~~3.~~[3] L.W. Miller, M.I. Tejedor-Tejedor, M.A. Anderson, Environ. Sci. & Tech. 33(12) (1999) 2070

~~4.~~[4] A. Sirisuk, C.G. Hill, M. A. Anderson, Catal. Today, 54 (1999) 159

~~5.~~[5] N. Negishi, T. Iyoda, K. Hashimoto, A. Fujishima, Chem. Lett. 9 (1995) 841

[6] M. Langlet, A. Kim, M. Audier, C. Guillard, J.M. Herrmann, J. Mater. Sci., 38 (2003) 394

~~7.~~[7] A. Dutschke, C. Diegelmann, P. Löbmann, Chem. Mater., 15 (2003) 3501

[8] H. Strohm, M. Sgraja, J. Bertling and P. Löbmann, J. Mater. Sci., 38 (2003) 1605

[9] A. Matsuda, Y. Kotani, T. Kogure, M. Tatsumisago, T. Minami, J. Amer. Ceramic Soc. 83(1) (2000) 229

[10] B. Sánchez, A. I. Cardona, M. Romero, P. Avila, A. Bahamonde, Catal. Today, 54 (1999) 369

[11] J. Shang, M. Chai, Y.F. Zhu, Environ. Sci. Tech., 37 (2003) 4494

Con formato: Numeración y viñetas

Con formato: Numeración y viñetas

[12] H. Zhang, J. F. Bandfield *J. Phys. Chem. B 104* (2000) 3481

[13] B. L. Bischoff, M. A. Anderson, Chem. Mater. 7 (1995) 1772

[14] Y. Li, T.J. White, S.H. Lim, J. Solid State Chem. 177(4-5) (2004) 1372

[15] K.N. Rao, Bull. Mater. Sci. 26 (2003) 239

[16] K.L. Yeung, S. T. Yau, A. J. Maira, J. M. Coronado, J. Soria, P. L. Yue, J. Catal. 219 (2003) 107–116

[17] C.H. Chen, E.M. Kelder, J. Schoonman, Thin Solid Films 342 (1999)

[18] C.C. Ting, S.-Y. Chen, D. M. Liu, J. Appl. Phys. 88(8) (2000) 4628

[19] G. M. Wallner, R.W. Lang, Solar Energy 79 (2005) 603

[20] K. Demeestere, A. De Visscher, J. Dewulf, M. Van Leeuwen, H. Van Langenhove Appl. Catal. B 54(4) (2004) 261

[21] H. Liu, S. Cheng, J. Zhang, C. Cao, W. Jiang, Chemosphere 35(12) (1997) 2881

[22] W. A. Jacoby, M. R. Nimlos, D. Blake, R. D. Noble, C.A. Koval, Environ. Sci. Technol., 28 (1994) 1661

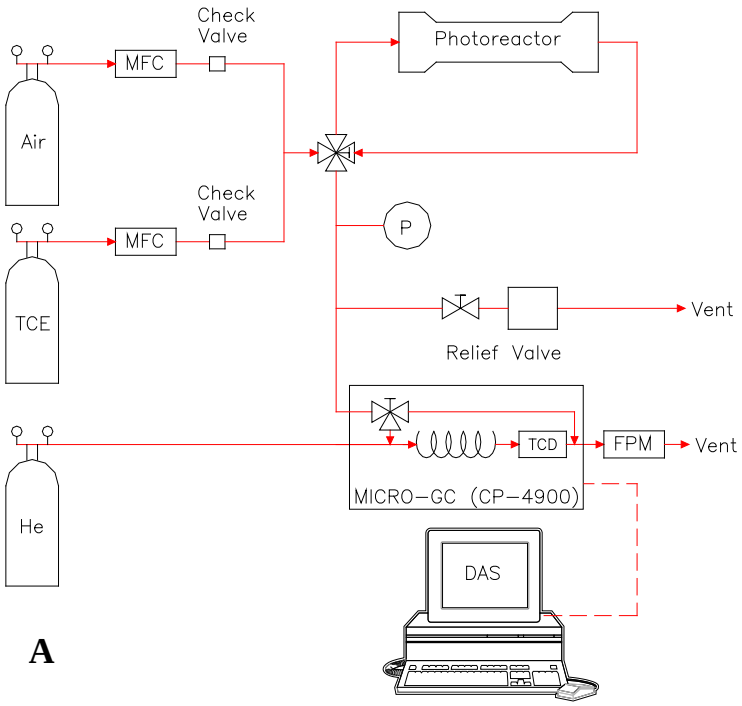

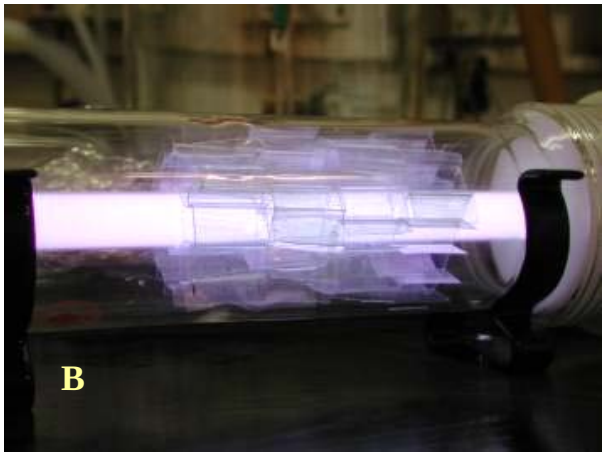

Figure 1. A) Scheme of the experimental set-up used for the photocatalytic assays and B) photograph of the photoreactor showing the arrangement of the PET monoliths around the UVA fluorescent lamp.

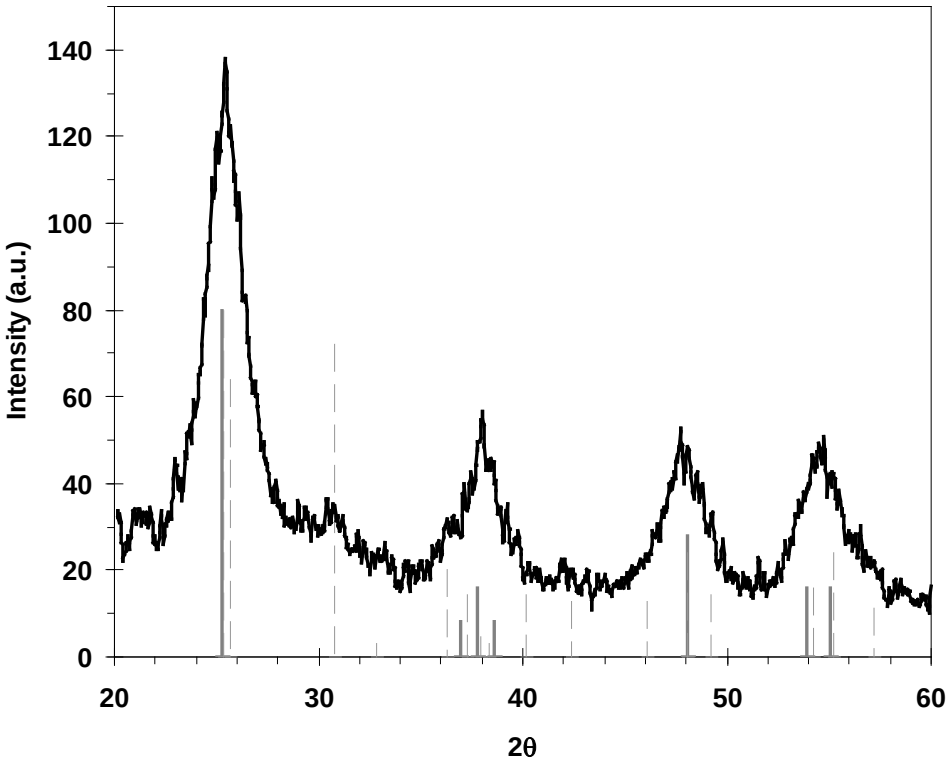

Figure 2. XRD pattern of the TiO_2 xerogel dried at RT. The marks at the bottom show the position of the reflection of anatase (solid) and brookite (dashed)

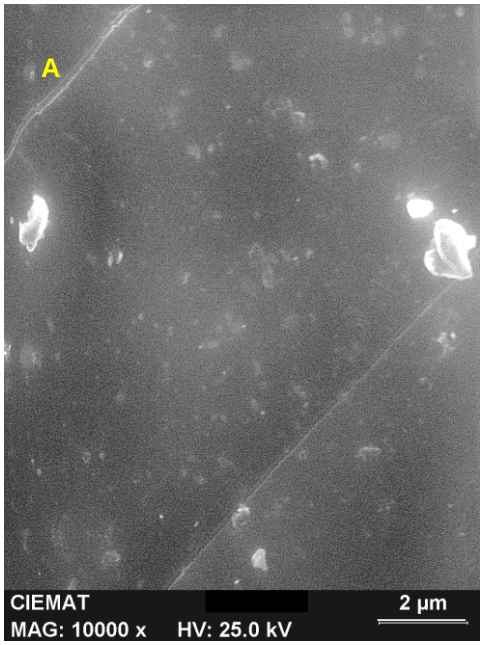

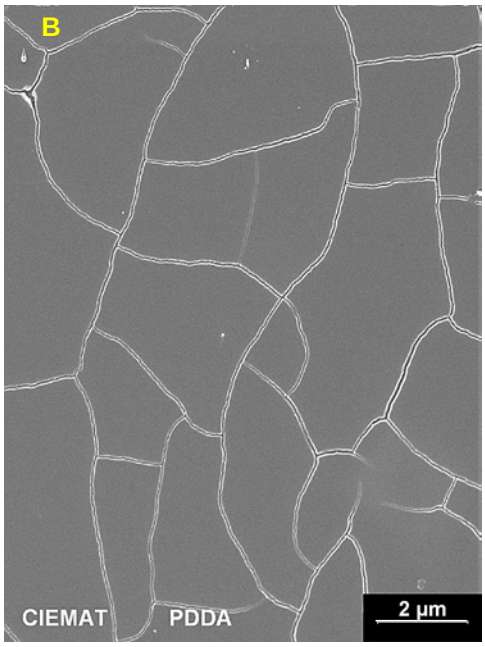

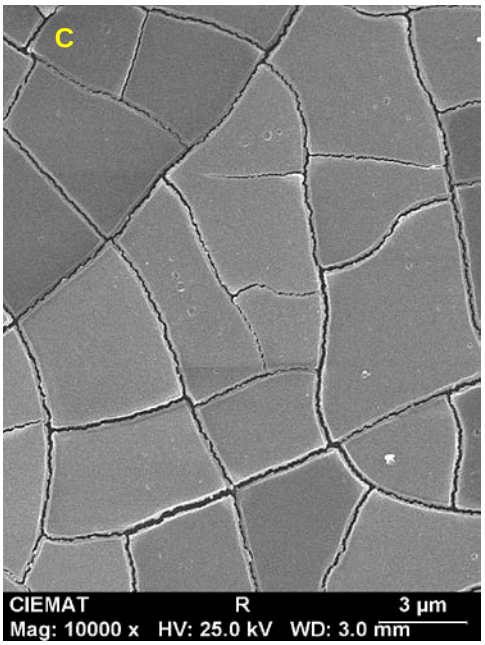

Figure·3. SEM micrographs of selected areas of the PET coated with A) TiO_2/SiO_2 (method A), B) PDDA and C) TiO_2/SiO_2/PDDA (method B).

Figure 4 A

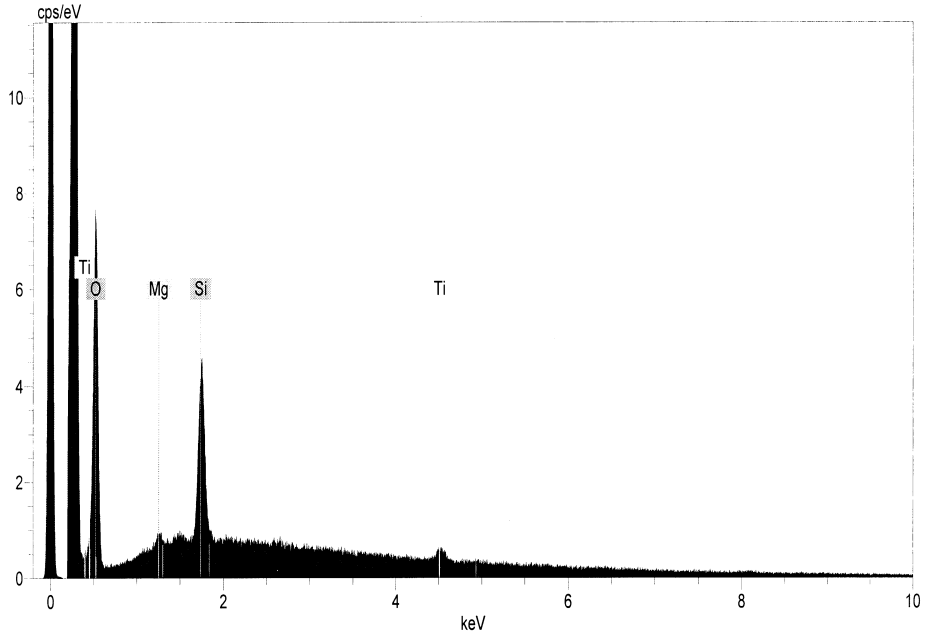

Figure 4B

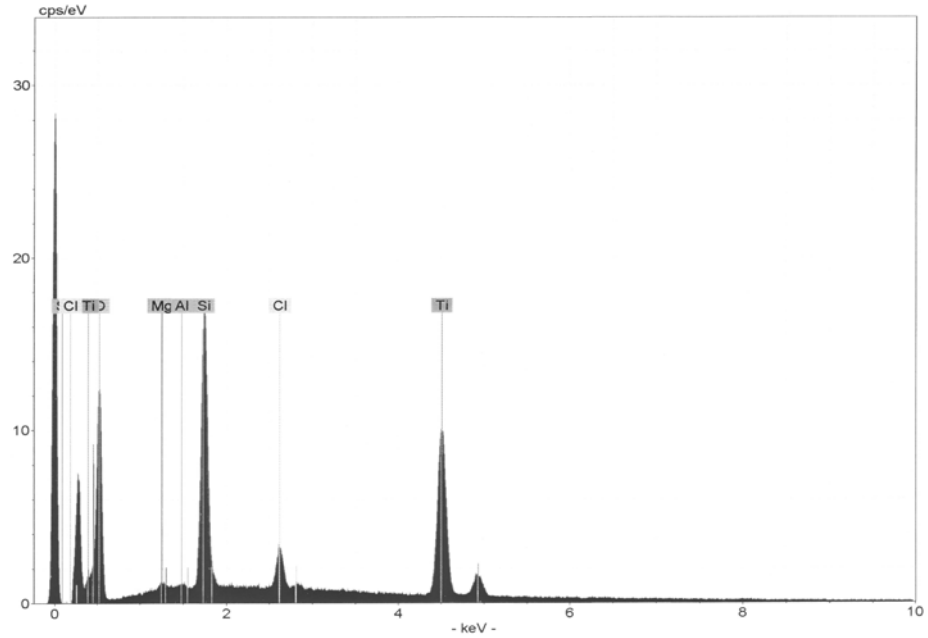

Figure 4. XED spectra of the PET monoliths coated with A) TiO_2/SiO_2 following procedure A, and B) TiO_2/SiO_2/PDDA (method B).

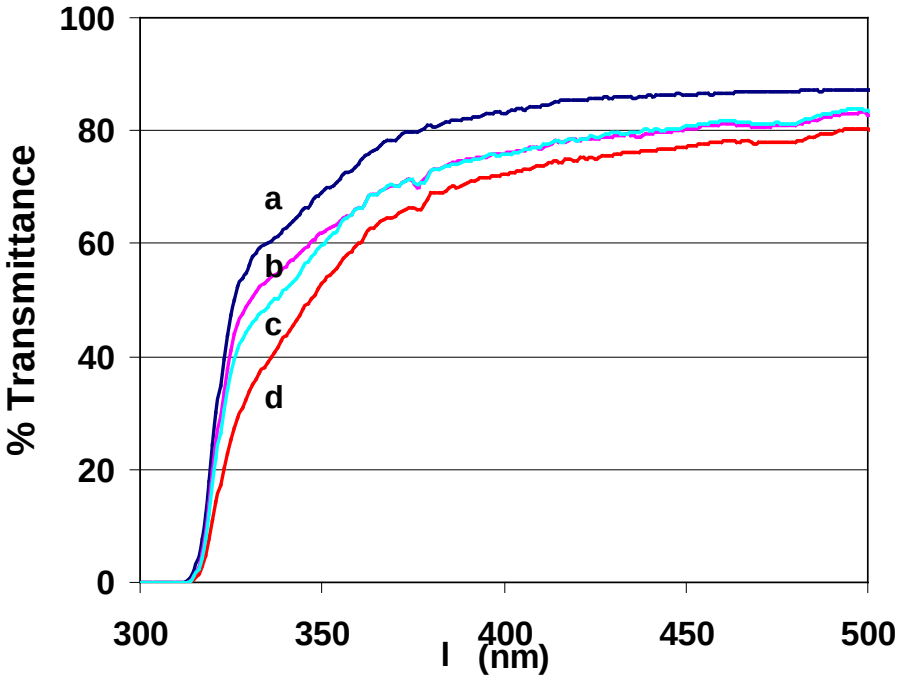

Figure 5. UV-vis transmittance spectra of the PET monoliths a) uncoated; b) coated with PDDA; c) TiO_2/SiO_2 (method A) and d)TiO_2/SiO_2/PDDA (method B).

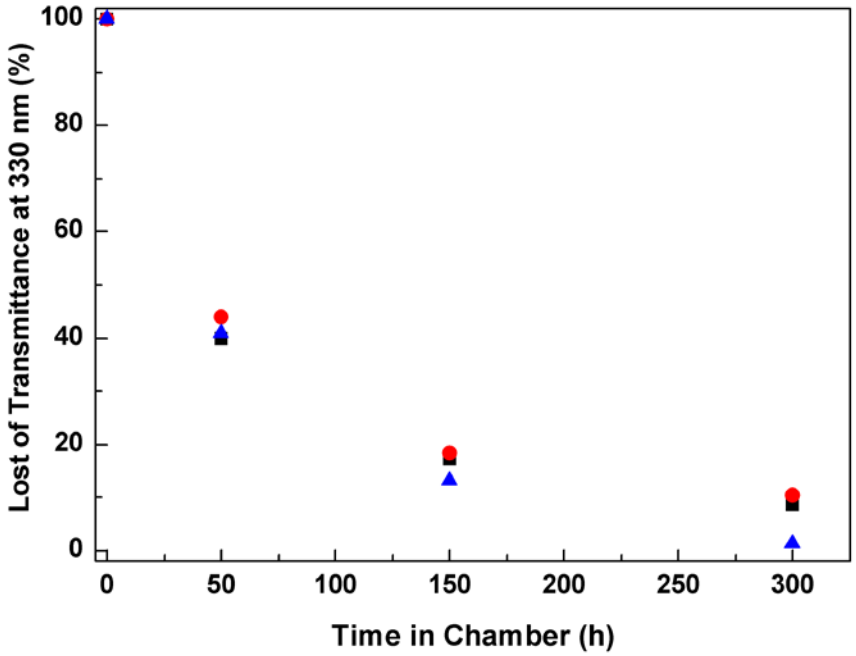

Figure 6. Variation of the transmittance of PET monoliths uncoated (circles); coated with TiO_2/SiO_2 (method A) (squares) and TiO_2/SiO_2/PDDA (method B) (diamonds) with the time in the weathering chamber.

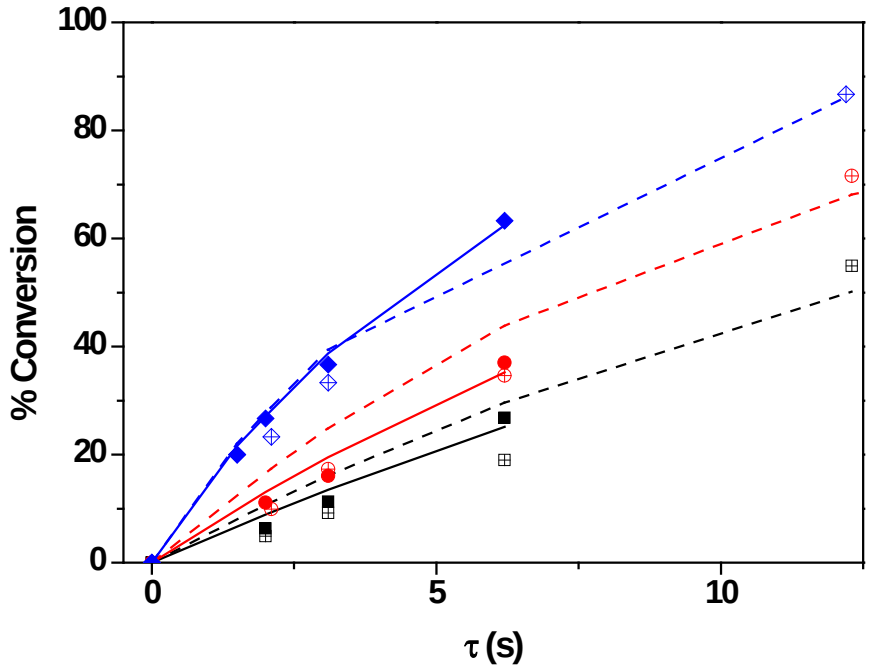

Figure 7. Variation of TCE conversion with residence time over the PET monoliths coated with TiO_2/SiO_2 prepared by procedure A (dashed lines) and B (solid lines). The initial TCE concentration was 30 (diamonds), 81 (circles) or 142 ppm_v (squares)

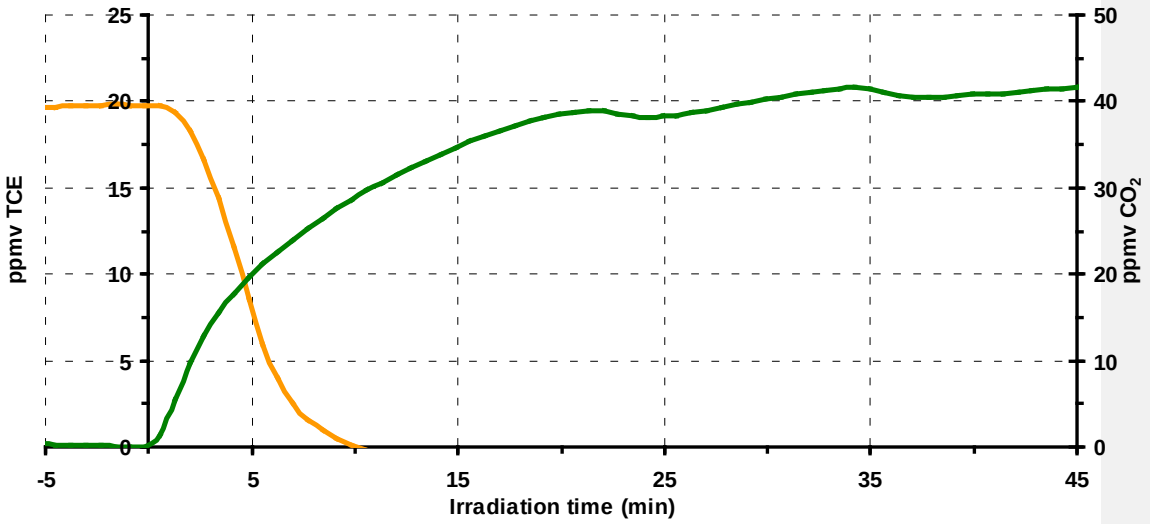
ppmv TCE
ppmv CO_2
Irradiation time (min)
25
20
15
10
5
0
50
40
30
20
10
0
-5
5
15
25
35
45

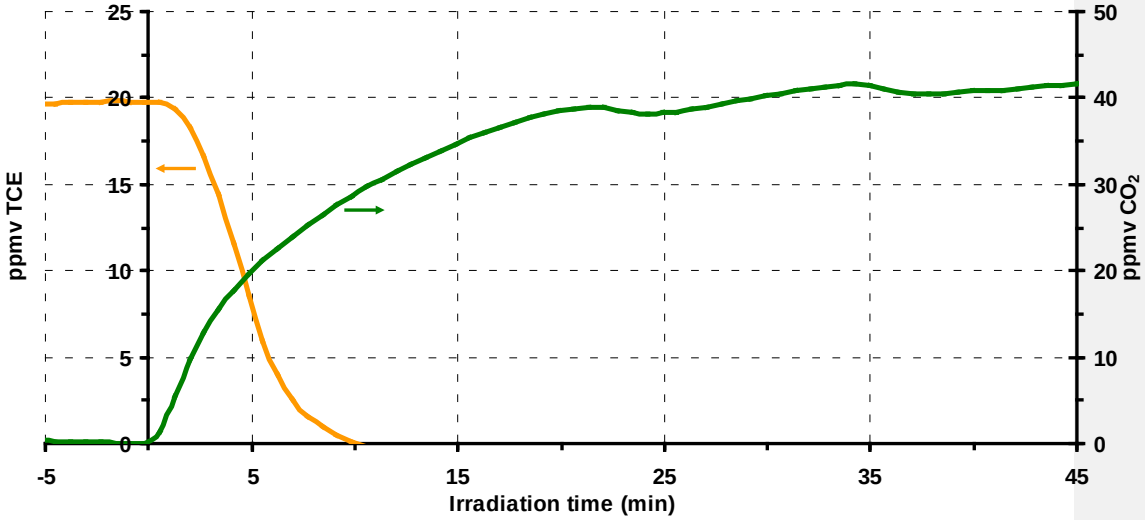
ppmv TCE
ppmv CO_2
Irradiation time (min)
25
20
15
10
5
0
50
40
30
20
10
0
-5
5
15
25
35
45

Figure 8. Evolution of the concentration of TCE and CO_2 with irradiation time over the TiO_2/PDDA/PET using a contact time of 21 s.